RSC Advances

PAPER

View Article Online
View Journal | View Issue

Cite this: *RSC Adv.*, 2015, **5**, 17660

Organosilicon functionalized glycerol carbonates as electrolytes for lithium-ion batteries†

Jinglun Wang,[a] Tianqiao Yong,[ab] Jianwen Yang,[c] Chuying Ouyang[d] and Lingzhi Zhang*[a]

Received 5th December 2014
Accepted 3rd February 2015

DOI: 10.1039/c4ra15854g

www.rsc.org/advances

Two triethoxyl-/trimethoxyl-silyl functionalized glycerol carbonates and one disiloxanyl functionalized glycerol carbonate were synthesized through a cycloaddition reaction of carbon dioxide with allyl glycidyl ether followed by a hydrosilylation with the corresponding hydrosilanes. Their chemical structures were fully characterized by ^{1}H and ^{13}C nuclear magnetic resonance (NMR) spectroscopy and their basic physicochemical properties including dielectric constant, viscosity, ionic conductivity, apparent lithium transference number and electrochemical window, were systematically measured. Trimethoxysilyl functionalized glycerol carbonate as electrolyte solvent with $LiPF_6$ (0.6 M) and lithium oxalyldifluoroborate (0.4 M) binary salts exhibited good cycling stability over 2.7–4.4 V in high-voltage-$LiCoO_2$/graphite full cells. Disiloxane functionalized glycerol carbonate acted as an efficient electrolyte additive to improve the wetting property on the separator in Li/$LiCoO_2$ cells.

1. Introduction

The current state-of-the-art $LiPF_6$-based carbonate electrolyte systems are commercially used in lithium-ion batteries, due to their high conductivity, excellent solubility with lithium salts, and ability to form a stable solid electrolyte interface (SEI), *etc.*[1,2] Research efforts have continued in an attempt to develop new electrolyte systems with fewer hazards and improved features concerning safety, operation voltage ranges, temperature limits, irreversible capacity, ion transportation, and so on.[3–5] However, organic carbonates are still an excellent choice as the solvent for electrolyte systems, and great advances have been documented for functional carbonates, such as fluoro functional carbonates,[6–9] vinyl functional carbonates,[10–13] and ionic liquid functional carbonates,[14] sulfonate functional carbonates,[15] alkyl functional carbonates,[16] and organosilicon functional carbonates,[17] as efficient electrolyte solvent/additive to address the problems mentioned above.

Organosilicon compounds have received much attention as electrolytes for energy storage devices due to their thermal and electrochemical stability, low flammability and environmentally benign characters.[18–23] On the other hand, it has also been reported that the electrochemical performances of lithium-ion batteries can be improved remarkably by adding a small amount of organosilicon additives to act as acid scavenger, flame retardant, over charge protecting agent, and SEI film-forming reagent in the conventional $LiPF_6$-based carbonate electrolytes.[24–27] Regarding organosilicon functional carbonates as electrolyte materials, a few research achievements have been documented over the past decades. For example, disiloxane functionalized carbonates were synthesized and characterized as a potential solvent/additive for electrolytes in lithium-ion batteries, although no cell tests were carried out for these compounds.[28,29] X. Huang *et al.* reported pentamethyldisiloxanylethylene and trimethylsilylethylene functionalized carbonate, EC-$CH_2CH_2Si(CH_3)_2$-$OSi(CH_3)_3$ and EC-$CH_2CH_2Si(CH_3)_3$, which showed efficient SEI forming capability on the surface of mesocarbon microbead anode.[30] Later, S. Tobishima and co-works studied EC-$CH_2CH_2Si(CH_3)_2OSi(CH_3)_3$ and heptamethyltrisiloxanylethylene functionalized carbonate (EC-CH_2CH_2-$Si(OSi(CH_3)_3)_2CH_3$) as electrolyte co-solvents for improving the cycling performance of lithium metal, graphite and Si–C anode.[31,32] We recently reported that trialkoxylsilyl compound with di(ethylene oxide) substituent (TESM2) in 1 M $LiPF_6$ exhibited good cycling stability in a $LiCoO_2$/Li half cell cycled over 3.0–4.35 V, retaining 90% capacity after 80 cycles. More recently, we reported a series of new organosilicon compounds containing nitrile and oligo(ethylene oxide) unit which showed an excellent cyclability with a discharge capacity of 152 mA h g^{-1} for 185 cycles at a higher cut-off voltage of 4.4 V in $LiCoO_2$/graphite full cell.[33,34]

[a]*CAS Key Laboratory of Renewable Energy, Guangzhou Institute of Energy Conversion, Chinese Academy of Sciences, Guangzhou 510640, China. E-mail: lzzhang@ms.giec.ac.cn; Fax: +86 20 37246026; Tel: +86 20 37246025*

[b]*University of Chinese Academy of Sciences, Beijing 100039, China*

[c]*College of Chemistry & Bioengineering, Guilin University of Technology, 12 Jiangan Road, Guilin, Guangxi, 541004, China*

[d]*Department of Physics, Jiangxi Normal University, Nanchang 330022, China*

† Electronic supplementary information (ESI) available: PFG-NMR fitting curves and comparison data of $LiCoO_2$/graphite performance in commercial electrolyte. See DOI: 10.1039/c4ra15854g

In this work, we introduce two triethoxyl-/trimethoxyl-silyl functionalized glycerol carbonates and one disiloxanyl functionalized glycerol carbonate as electrolyte solvent and additive for the application of lithium-ion batteries. The electrochemical performances of trimethoxylsilyl functionalized glycerol carbonate and disiloxanyl functionalized glycerol carbonate have been investigated as electrolyte solvent and additive for high-voltage application (upper cut-off voltage of 4.4 V) in $LiCoO_2$/graphite full cells and for improving wetting property on the separator in Li/$LiCoO_2$ half cells, respectively.

2. Experimental

2.1. Materials

Trimethoxysilane, triethoxysilane, 1,1,1-trimethyl-2,2-dimethyldisiloxane and *N*-methyl-2-pyrrolidone (NMP, Aladdin Reagent Co., China), ethylene carbonate (EC, Shanshan Co., China) and dimethyl carbonate (DMC, Shanshan Co., China), and $LiPF_6$ (Guangzhou Tinci High-Tech Materials Co., China) were used as received. Artificial graphite powder and $LiCoO_2$ powder were obtained from Amperex Technology Limited (China). A Celgard 2400 microporous polypropylene membrane was used as the separator.

2.2. Apparatus

^{1}H NMR, ^{13}C NMR, and PFG-NMR experiments were taken on a Bruker Avence 400 spectrophotometer in $CDCl_3$. Viscosity (η) measurements were tested on SPb-2 Viscometer (Nirun Intelligent Technology Co., Ltd.). The dielectric constants (ε) were measured on an 870 Liquid Dielectric Constant Meter (Scientifica). Ionic conductivities were determined by DDS-310 conductivity instrument, variable temperature conductivity measurements were conducted in an oil bath for temperature ranging between 0 °C and 90 °C. Linear scanning voltammograms measurements were performed on a platinum working electrode, with counter and reference electrodes of lithium foils using an electrochemical workstation (BAS-ZAHNER IM6, Germany) with the scanning rate of 5 mV s^{-1} between −0.5 to 6.7 V. The static contact angle measurements were taken by a CCD camera on Dataphysics OCA40 Micro.

2.3. Synthesis

General procedure: (1) carbon dioxide (3 MPa) was purged into a 100 mL stainless steel autoclave which was placed with allyl glycidyl ether (0.2 mol) and tetra-butylammonium bromide (0.02 mol), and the reaction mixture was stirring for 16 hours at 80 °C. After the reaction was completed, the reactor was quickly cooled to 0 °C in ice water, the excess of CO_2 was depressurized slowly. The resulting mixture was distilled under vacuum condition giving allyl glycerol carbonate (AGC) with a purity of 99% and a yield of 95%. (2) The synthesized AGC (0.2 mol) was added slowly to silane (0.2 mol, trimethoxysilane, triethoxysilane, or pentamethyldisiloxane) with PtO_2 (1 wt%) as catalyst. After stirring at 60 °C for 12 h, the product was obtained by fractional distillation. The obtained organosilicon functionalized glycerol carbonate was dried over with CaH_2 and stored with 4 Å molecular sieves. These compounds had a water content of approximately 17 ppm as measured by coulometric Karl Fischer titration (Model 831, Metrohm). The NMR data are as followed:

TMGC. ^{1}H NMR (600 MHz, $CDCl_3$): δ 0.63 (m, 2H, $(CH_3O)_3SiCH_2$), 1.66 (m, 2H, $SiCH_2CH_2$), 3.47 (m, 2H, $CH_2CH_2CH_2$), 3.56 (s, 9H, $(CH_3O)_3Si$), 3.63 (dd, 2H, $-CH_2CH_2CH_2OCH_2$), 4.38 (q, 1H, $CHCH_2O$), 4.48 (q, 1H, $CHCH_2O$), 4.78 (q, 1H, $CHCH_2O$); ^{13}C NMR (150.9 MHz, $CDCl_3$): δ 5.06, 22.65, 50.51, 66.29, 69.57, 73.89, 75.05, 154.96.

TEGC. ^{1}H NMR (600 MHz, $CDCl_3$): δ 0.62 (m, 2H, $(CH_3CH_2O)_3SiCH_2$), 1.22 (t, 9H, $^3J = 7.2$ Hz, $(CH_3CH_2O)_3Si$), 1.68 (m, 2H, $SiCH_2CH_2$), 3.48 (m, 2H, $SiCH_2CH_2CH_2$), 3.63 (dd, 2H, $-CH_2CH_2CH_2OCH_2$), 3.80 (q, 6H, $^3J = 7.2$ Hz, $(CH_3CH_2O)_3Si$), 4.39 (q, 1H, $^3J = 8.4$ Hz, $OCHCH_2O$), 4.48 (q, 1H, $^3J = 8.4$ Hz, $OCHCH_2O$), 4.79 (m, 1H, $OCHCH_2O$). ^{13}C NMR (150.9 MHz, $CDCl_3$): δ 6.37, 18.28, 22.88, 58.39, 66.33, 69.57, 74.13, 74.99, 154.89.

DSGC. ^{1}H NMR (600 MHz, $CDCl_3$): δ 0.05 (s, 6H, $OSi(CH_3)_2$), 0.06 (s, 9H, $-Si(CH_3)_3$), 0.49 (m, 2H, $OSi(CH_3)_2CH_2$), 1.59 (m, 2H, $OSi(CH_3)_2CH_2CH_2$), 3.46 (m, 2H, $-CH_2CH_2CH_2O$), 3.64 (dd, 2H, $-CH_2CH_2CH_2OCH_2$), 4.39 (q, 1H, $CHCH_2O$), 4.49 (q, 1H, $CHCH_2O$), 4.80 (q, 1H, $CHCH_2O$). ^{13}C NMR (150.9 MHz, $CDCl_3$): δ 0.24, 1.95, 14.09, 23.31, 66.34, 69.58, 74.79, 75.06, 154.94.

2.4. Pulsed magnetic-field gradient-NMR (PFG-NMR)

The solutions for PFG-NMR analysis was prepared through dissolving 0.5 M LiTFSI into the synthesized organosilicon functionalized glycerol carbonates. The samples were transferred into the coaxial NMR tubes, and the diffusion coefficients of the cationic and anionic species were measured by the application of the PFG-NMR technique at 25 °C.[35]

2.5. Electrode preparation and cell tests

Working electrodes were prepared by mixing $LiCoO_2$, carbon black and polyvinylidene fluoride (PVDF) at a weight ratio of 90 : 5 : 5 in NMP, then the slurry was spread onto an Al foil and dried at 80 °C under vacuum for 6 h. The graphite anodes were made by coating a mixture of graphite, carbon black and PVDF with weight ratio 90 : 5 : 5 on copper foil. The 2025 type coin cells were assembled for electrochemical tests under a dry argon atmosphere in the glove box (Mikrouna, H_2O and O_2 < 1 ppm). The $LiCoO_2$/graphite full cells were galvanostatically charged and discharged with the current density of C/10 in a voltage range of 2.7–4.4 V, the $LiCoO_2$/Li half cells were galvanostatically charged and discharged on a multi-channel battery test system (NEWARE BTS-610) in a voltage range of 2.7–4.2 V.

3. Results and discussion

3.1. Synthesis of organosilicon functionalized glycerol carbonate

Considering the availability of the starting material, glycerol carbonate which can be obtained through an environmental friend route from biomass was chose as a starting material rather than butylene carbonate.[30–32] On the other side, the traditional phosgene route for the synthesis of cyclic carbonates

has been replaced by cycloaddition of carbon dioxide with epoxides in the view point of carbon dioxide chemical fixation and sustainable chemistry.[36,37] Therefore, the target organosilicon functionalized glycerol carbonates have been efficiently synthesized through a two-step route of cycloaddition carbon dioxide with allyl glycidyl ether to generate allyl glycerol carbonate (AGC), followed by hydrosilylation of AGC with corresponding hydrosilanes (Scheme 1, denoted as TMGC, TEGC, and DSGC). Compared with the reported methodologies, esterification of 3-(allyloxy)-propane-2,2-diol with linear carbonate followed by hydrosilylation with hydrosilanes[28] or by hydrosilylation of a laborious synthesized butylene carbonate with hydrosilanes,[32] the two-step route is undoubtedly the most efficient for preparing organosilicon functionalized carbonate. The synthesized organosilicon functionalized glycerol carbonates with the overall yield over 90% are colourless and clear liquid at room temperature and are characterized through ^{1}H NMR and ^{13}C NMR.

3.2. Physicochemical and electrochemical properties

The physical properties for these compounds, such as dielectric constant (ε), viscosity (η), and ionic conductivity (σ) are collected in Table 1. It seems that the introduction of organosilicon group into the framework of AGC results in decreasing their ε and increasing their η compared with those of AGC. The value of their dielectric constants decrement in the order of $\varepsilon_{AGC} > \varepsilon_{TMGC} > \varepsilon_{TEGC} > \varepsilon_{DSGC}$ (with increasing volume of silicon functional group) and the value of their viscosities decline in the order of $\eta_{DSGC} > \eta_{TMGC} > \eta_{TEGC} > \eta_{AGC}$ (exhibiting similar viscosity to the reported siloxane functionalized butylene cyclic carbonate (4-(2-trimethylsilyloxydimethylsilylethyl)-1,3-dioxolan-2-one), 18.0 mPa S, 20 °C (ref. 32)). Usually, high dielectric constant facilitates the dissociation of lithium salts, thus improving ionic conductivity; while high viscosity limits the mobility of Li^{+} and decreases the ionic conductivity. It is easy to understand that the value of their ionic conductivity decrease in the order of $\sigma_{AGC} > \sigma_{TEGC} > \sigma_{TMGC} > \sigma_{DSGC}$, TEGC has the higher conductivity than that of TMGC probably because viscosity dominates the conductivity for these organosilicon functionalized glycerol carbonates ($\eta_{TMGC} > \eta_{TEGC}$). DSGC has the lowest conductivity for its higher viscosity and lower dielectric constant than TMGC and TEGC. As a consequence, these organosilicon functionalized glycerol carbonate compounds have somewhat lower conductivities than the conventional electrolytes, *e.g.* propylene carbonate has conductivity value of 5.1 mS cm^{-1} with LiTFSI.[38]

In order to analyze the mechanism of ionic conduction, the ionic conductivity dependence on temperature was studied in the temperature range of 273–363 K. Fig. 1a shows the Arrhenius plot of temperature dependent conductivity (ln σ) *versus* the inverse absolute temperature for the organosilicon functionalized glycerol carbonates. From the Arrhenius plot, it can be seen that the ionic conductivity shows curvature indicating that Vogel–Tammann–Fulcher (VTF) behavior is involved. Usually, VTF behavior is valid for polymer and glassy

Table 1 Physicochemical parameters of organosilicon functionalized glycerol carbonate[a]

Compound	ε	η/mPa S	σ^{b}/ mS cm^{-1}	σ_o/ S cm^{-1}	E_a/ KJ mol	T_0/K
AGC	71.1	7.4	1.09	1.45	3.89	190.6
TMGC	37.8	12.8	0.49	1.22	4.35	188.6
TEGC	31.6	12.5	0.59	1.56	4.71	189.1
DSGC	25.8	14.9	0.07	0.76	5.90	187.8

[a] Dates are measured at room temperature. [b] Doping with 1 M LiTFSI.

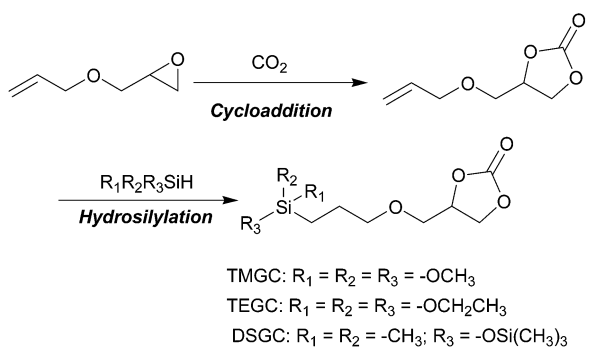

Scheme 1 The synthetic route for organosilicon functionalized glycerol carbonate.

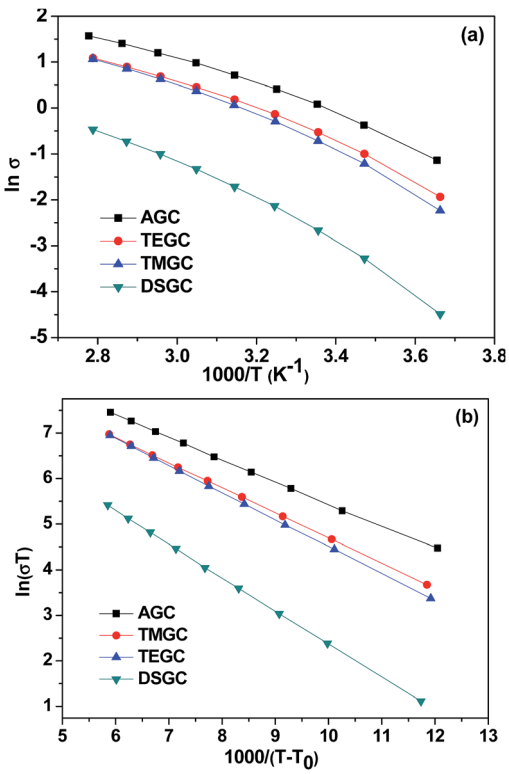

Fig. 1 (a) Arrhenius plots of conductivity *versus* temperature for organosilicon functionalized glycerol carbonates with 1 M LiTFSI. (b) Vogel–Tammann–Fulcher (VTF) plots of conductivity *versus* temperature for organosilicon functionalized glycerol carbonates with 1 M LiTFSI.

electrolytes, or concentrated electrolyte solutions,[39] and has also been widely observed for organosilicon functionalized electrolytes.[40] The $\ln(\sigma T)$ *versus* $(T - T_0)^{-1}$ plots of the organosilicon functionalized glycerol carbonates fit well linearly (Fig. 1b) according to the VTF eqn (1):

$$\sigma = \sigma_o T^{-1/2} \exp[-E_a/R(T - T_0)] \quad (1)$$

where σ_o, E_a and T_0 is derived from the VTF equation and listed in Table 1. σ_o and E_a are parameters correlated to the charge carrier number and the activation energy, respectively, whereas T_0 represents the ideal glass transition temperature. The VTF diagrams exhibits a linear behaviour with a higher slope for the DSGC–LiTFSI solution among the functionalized carbonate family, suggesting that DSGC–LiTFSI mixture possesses higher activation energy for the ion transport resulting in slower transport property.

PFG-NMR tests of ^{7}Li and ^{19}F ($TFSI^-$) was carried out to measure the diffusion coefficients of Li^+ and $TFSI^-$. The diffusion coefficients of ^{7}Li and ^{19}F were determined according to the relation:

$$I = I_{[0]} \times \exp[-D \times (2 \times \pi \times \gamma \times G \times \delta)^2 \times (\Delta - \delta/3)] \quad (2)$$

where γ is the gyromagnetic ratio, D is the diffusion coefficient, δ is the pulse width of the field width of the field gradient, G denotes the magnetic field gradient, and Δ is the duration time. Then the diffusion coefficient values could be obtained by fitting the intensity data $I(G)$ by eqn (2) (the fitting curves are displayed in ESI, Fig. S1†). Several author related the self coefficient to the Stokes–Einstein eqn (3):

$$D = K_B T/(c\pi\eta r) \quad (3)$$

where η represents the viscosity, r is the effective hydrodynamics radius. The constant c varies between 4 and 6, depending on the shape of the diffusing entity. As illustrated in Table 2, the diffusion coefficients of $TFSI^-$ are generally large than those of the Li^+ despite the smaller size of Li^+. Thus, the solvation of the Li^+ can be assumed. The diffusion coefficient of anion in the organosilicon functionalized glycerol carbonates are correlated to the variation of their viscosity ($\eta_{AGC} > \eta_{TEGC} > \eta_{TMGC} > \eta_{DSGC}$), while the diffusion coefficient of cation may correlate to the variation of their viscosity and the coordinated solvent radius ($r_{DSGC} > r_{TEGC} > r_{TMGC} > r_{AGC}$).

In order to analyze the individual contributions of the cation and anion to the overall ionic conductivity of the mixture, the apparent lithium-ion transference number (t_{Li^+}) could be calculated by eqn (4):

$$t_{Li^+} = D_{Li^+}/(D_{Li^+} + D_{F^-}) \quad (4)$$

It has been found that the t_{Li^+} increased in the order $t_{Li^+/AGC} < t_{Li^+/DSGC} < t_{Li^+/TEGC} < t_{Li^+/TMGC}$ (in Table 2). Although possessing the highest dielectric constant, lowest viscosity, and the resulting highest ionic conductivity, AGC exhibits the lowest t_{Li^+} of the four compounds, which may originate from the complexation ability of the C=C double bond with Li^+, thus inhibiting the mobility of Li^+.

The electrochemical stability windows (ESW) of the synthesized compounds with 1 M LiTFSI salt were determined by linear sweep voltammetry (Fig. 2). TMGC, TEGC, and DSGC compounds oxidatively decomposes at around 4.8 V (*vs.* Li/Li^+), except for AGC at 5.8 V. The trend in reductive degradation of these compounds increases in the order of TMGC < TEGC ≅ AGC < DSGC. Based on their physicochemical and electrochemical data, these organosilicon functionalized glycerol carbonate compounds are possible to be used as electrolyte solvent or additive for lithium-ion batteries.

3.3. TMGC as electrolyte solvent

The high voltage performance for lithium-ion batteries using $LiCoO_2$ as the cathode and artificial graphite as the anode was investigated using TMGC as electrolyte solvent owing to its high electrochemical window, high apparent lithium transference number and moderate ionic conductivity. 0.4 M lithium oxalyldifluoroborate (LiODFB) and 0.6 M $LiPF_6$ are chosen as the binary lithium slats because LiODFB provides an effective passivation film on the graphite anode and $LiPF_6$ exhibits a good dissolving property in organosilicon functionalized glycerol carbonate. The cycling performance of graphite/0.4 M LiODFB + 0.6 M $LiPF_6$ in TMGC/$LiCoO_2$ full cells with a high cut-off voltage of 4.4 V is plotted in Fig. 3. The cell was charged and discharged at a rate of C/10 and cycled between 2.7 and 4.4 V at room temperature. It

Table 2 Results of the PFG-NMR measurements

	D_{Li^+}	D_{F^-}	t_{Li^+}
AGC	3.253×10^{-12} m^2 s^{-1}	6.420×10^{-12} m^2 s^{-1}	0.336
TMGC	3.012×10^{-12} m^2 s^{-1}	3.666×10^{-12} m^2 s^{-1}	0.451
TEGC	2.332×10^{-12} m^2 s^{-1}	4.064×10^{-12} m^2 s^{-1}	0.365
DSGC	1.844×10^{-12} m^2 s^{-1}	3.482×10^{-12} m^2 s^{-1}	0.346

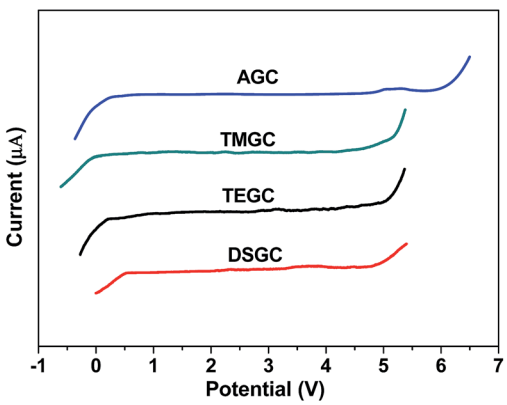

Fig. 2 Linear scanning voltammograms of the electrolytes with 1 M LiTFSI in the organosilicon functionalized glycerol carbonates.

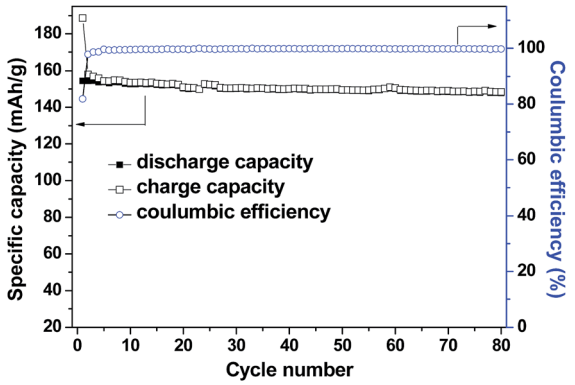

Fig. 3 Cycling performance of graphite/$LiCoO_2$ full cell with 0.4 M LiODFB + 0.6 M $LiPF_6$ in TMGC as electrolyte at C/10 with a high cut-off voltage of 4.4 V.

exhibits excellent cycling performance with discharge capacity over 148 mA h g^{-1} after 80 cycles, while the cell using conventional electrolyte of 1 M $LiPF_6$ in EC/DEC/DMC (1/1/1, in vol) fades quickly (showed in ESI, Fig. S2†). The low discharge capacity may relate to the high viscosity of the electrolyte, which needs optimization near future.

3.4. DSGC as electrolyte additive

Among the merits of organosilicon compounds mentioned above, another unique property is their extraordinary low surface free energy of siloxane compounds (surface tension of hexamethyldisiloxane is 16 mN m^{-1}),[41] so that they have been widely used as surface active agents for surface treatment. The polyether modified siloxanes was reported as an electrolyte additive for improving the surface film stability on Li metal electrode.[42] In this study, the wetting property of DSGC in the electrolyte of 1 M $LiPF_6$ in EC/DEC (1/1, in vol) was investigated by static contact angle measurement. The static contact angle of the electrolyte with/without the addition of 5 vol% DSGC on electrode is too small to be measured (the electrolyte spreads over quickly on the surface of $LiCoO_2$ electrode). However, we found that the electrolyte with an optimized amount of 5 vol% DSGC showed a smaller contact angle (35.2°) on separator compared with 46.2° for the electrolyte without the addition of DSGC (Fig. 4), indicating the efficient wetting capability on separator for DSGC as additive in electrolyte. It is well known that the separator placed between cathode and anode is one of critical components in lithium-ion batteries, which could effectively transport ionic charge carriers as well as to prevent the electric contact between two electrodes.[43,44] In our experiments, the electrolyte with 5 vol% DSGC in Li/$LiCoO_2$ cells exhibited higher capacities at high rate conditions, *e.g.* 63 mA h g^{-1} at 5 C as compared with 0.7 mA h g^{-1} for the cell without DSGC additive. When cycled at 0.5 C after 5 C tests, the cells fully recovered its capacity to the former 0.5 C level of about 120 mA h g^{-1} (Fig. 5a and b). The electrochemical impedance spectroscopy (EIS) measurements of the cells with/without

Fig. 4 Static contact angle measurement on separator with different electrolytes, without addition of DSGC (left) and with addition of DSGC (right).

DSGC additive after C-rate test under the charged state at the voltage of 4.2 V are provided in Fig. 6. All the Nyquist plots are composed of two partially overlapping semi-circles at high and medium frequency range and a straight sloping line at the low frequency end, representing respectively three resistance components: film resistance, charge transfer resistance, and Li^+ diffusion resistance.[45] The radii of the two semi-circles were much smaller than those without DSGC, indicating the lower surface film resistance and charge transfer resistance for the cells with DSGC in the electrolyte. Therefore, the improved rate performances for the electrolyte with 5 vol% DSGC can be attributed to this improved wetting on separator by DSGC and the correspondingly enhanced kinetics.

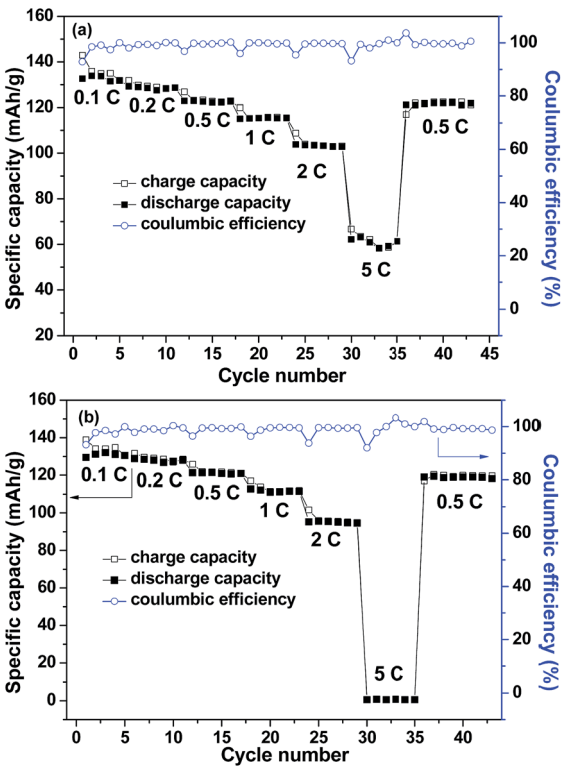

Fig. 5 C-rate performances and coulombic efficiency of Li/$LiCoO_2$ cells in different electrolytes (a) with DSGC, (b) without DSGC in the voltage range of 2.7–4.2 V.

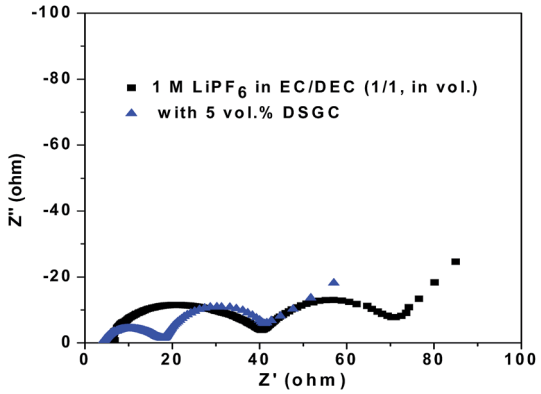

Fig. 6 EIS impedance of Li/$LiCoO_2$ cell after C-rate tests with or without DSGC addition.

4. Conclusions

Two triethoxyl-/trimethoxyl-silyl functionalized glycerol carbonates and one disiloxanyl functionalized glycerol carbonate were synthesized under mild conditions with high yield by cycloaddition carbon dioxide with allyl glycidyl ether to form allyl glycerol carbonate, followed by hydrosilylation with corresponding hydrosilanes. Although the dielectric constant, viscosity, and ionic conductivity decreased with the introduction of organosilicon group, the apparent lithium transference number increased compared with allyl glycerol carbonate. Trimethoxyl-silyl functionalized glycerol carbonate in 0.4 M LiODFB + 0.6 M $LiPF_6$ binary salts showed better cycling performance compared with the conventional electrolyte (1 M $LiPF_6$ in EC/DEC/DMC, 1/1/1 in vol) at a cut-off voltage of 4.4 V in graphite/$LiCoO_2$ full cells. Disiloxanyl functionalized glycerol carbonate with 5 vol% content in the electrolyte of 1 M $LiPF_6$ in EC/DEC (1/1 in vol) improved significantly wetting property on the separator, and thus improved rate performance in Li/$LiCoO_2$ half cells. These results demonstrate that these organosilicon functionalized glycerol carbonates have considerable potential as electrolyte solvent/additive for use in lithium-ion batteries.

Acknowledgements

This work is supported by the Hundred Talents Program of Chinese Academy of Sciences (CAS), the National Natural Science Foundation of China (50973112/21202165), Cooperative Innovation Project of Science & Technology of Guangzhou (201423), Collaboration Project of CAS-Guangdong Province (2013B091300017), and Guangzhou Municipal Project for Science & Technology (2014Y2-00219).

Notes and references

1 V. Etacheri, R. Marom, R. Elazari, G. Salitra and D. Aurbach, *Energy Environ. Sci.*, 2011, **4**, 3243–3262.
2 K. Xu, *Chem. Rev.*, 2004, **104**, 4303–4417.
3 T. R. Jow, K. Xu, O. Borodin and M. Ue, *Electrolytes for Lithium and Lithium-Ion Batteries*, ed. M. Ue, Y. Sasaki, Y. Tanaka, M. Morita and K. Abe, Springer, 2014, ch. 2 and 3, pp. 112–226.
4 S. S. Zhang, *J. Power Sources*, 2006, **162**, 1379–1394.
5 K. Xu, *Chem. Rev.*, 2014, **114**(23), 11503–11618.
6 Z. C. Zhang, L. Hu, H. Wu, W. Weng, M. Koh, P. C. Redfern, L. A. Curtiss and K. Amine, *Energy Environ. Sci.*, 2013, **6**, 1806–1810.
7 M. H. Ryou, G. B. Han, Y. M. Lee, J. N. Lee, D. J. Lee, Y. O. Yoon and J. K. Park, *Electrochim. Acta*, 2010, **55**, 2073–2077.
8 T. Achiha, T. Nakajima, Y. Ohzawa, M. Koh, A. Yamauchi, M. Kagawa and H. Aoyama, *J. Electrochem. Soc.*, 2010, **157**, A707–A712.
9 Y. Zhu, M. D. Casselman, Y. Li, A. Wei and D. P. Abraham, *J. Power Sources*, 2014, **246**, 184–191.
10 L. E. Ouatani, R. Dedryvere, C. Siret, P. Biensan, S. Reynaud, P. Iratcabal and D. Gonbeau, *J. Electrochem. Soc.*, 2009, **156**, A103–A113.
11 F. Martin, J. Morales and L. Sanchez, *ChemPhysChem*, 2008, **9**, 2610–2617.
12 E. G. Shim, T. H. Nam, J. G. Kim, H. S. Kim and S. I. Moon, *Electrochim. Acta*, 2007, **53**, 650–656.
13 G. Chen, G. V. Zhuang, T. J. Richardson, G. Liu and P. N. Ross, *Electrochem. Solid-State Lett.*, 2005, **8**, A344–A347.
14 T. Tsuda, K. Kondo, T. Tomioka, Y. Takahashi, H. Matsumoto, S. Kuwabata and C. L. Hussey, *Angew. Chem., Int. Ed.*, 2011, **50**, 1310–1313.
15 LG CHEM LTD, WO Pat., 035 928, 2008.
16 H. Zhao, S. J. Park, F. F. Shi, Y. B. Fu, V. Battaglia, P. N. Ross Jr and G. Liu, *J. Electrochem. Soc.*, 2014, **161**, A194–A200.
17 T. Nakanishi, M. Kashida, S. Miyawaki, S. Ichinobe and M. Aramata, *US Pat.*, 0 0839 992, 2006.
18 N. A. A. Rossib and R. West, *Polym. Int.*, 2009, **58**, 267–277.
19 K. Y. Tse, L. Z. Zhang, S. E. Baker, B. M. Nichols, R. West and R. J. Hamers, *Chem. Mater.*, 2007, **19**, 5734–5741.
20 W. Weng, Z. C. Zhang, J. Lu and K. Amine, *Chem. Commun.*, 2011, **47**, 11969–11971.
21 L. Z. Zhang, Z. C. Zhang, S. Harring, M. Straughan, M. Butorac, Z. H. Chen, L. J. Lyons, K. Amine and R. West, *J. Mater. Chem.*, 2008, **18**, 3713–3717.
22 L. Z. Zhang, L. Lyons, J. Newhouse, Z. C. Zhang, M. Straughan, Z. H. Chen, K. Amine, R. J. Hamers and R. West, *J. Mater. Chem.*, 2010, **20**, 8224–8226.
23 K. Amine, Q. Z. Wang, D. R. Vissersa, Z. C. Zhang, N. A. A. Rossib and R. West, *Electrochem. Commun.*, 2006, **8**, 429–433.
24 Q. Xia, B. Wang, Y. P. Wu, H. J. Luo and T. van Ree, *J. Power Sources*, 2008, **180**, 602–606.
25 K. Takechi and T. Shiga, *US Pat.*, 6 235 341, 2001.
26 H. P. Zhang, Q. Xia, B. Wang, L. C. Yang, Y. P. Wu, D. L. Sun, C. L. Gan, H. J. Luo, A. W. Bebeda and T. van Ree, *Electrochem. Commun.*, 2009, **11**, 526–529.
27 M. Walkowiak, D. Waszak, G. Schroeder and B. Gierczyk, *Electrochem. Commun.*, 2008, **10**, 1676–1679.

28 T. West, K. Amine, Z. C. Zhang, Q. C. Wang, N. A. A. Rossi and D. R. Vissers, *US Pat.*, 0 170 254, 2005.
29 N. A. A. Rossi, Q. Z. Wang, K. Amine and R. West, *Silicon*, 2010, **2**, 201–208.
30 X. J. Wang, H. S. Lee, H. Li, X. Q. Yang and X. J. Huang, *Electrochem. Commun.*, 2010, **12**, 386–389.
31 Y. Takei, K. Takeno, H. Morimoto and S. Tobishima, *J. Power Sources*, 2013, **228**, 32–38.
32 T. Takeuchi, S. Noguchi, H. Morimoto and S. Tobishima, *J. Power Sources*, 2010, **195**, 580–587.
33 X. Y. Qin, J. L. Wang, Y. J. Mai, D. P. Tang, X. Y. Zhao and L. Z. Zhang, *Ionics*, 2013, **19**, 1567–1572.
34 T. Q. Yong, J. L. Wang, Y. J. Mai, X. Y. Zhao, H. Luo and L. Z. Zhang, *J. Power Sources*, 2014, **254**, 29–32.
35 D. Wu, A. Chen and C. S. Johnson, *J. Magn. Reson., Ser. A*, 1995, **115**, 260–264.
36 T. Sakakura and K. Kohno, *Chem. Commun.*, 2009, 1312–1330.
37 C. X. Miao, J. Q. Wang, Y. Wu, Y. Du and L. N. He, *ChemSusChem*, 2008, **1**, 236–241.
38 M. Ue and S. Mori, *J. Electrochem. Soc.*, 1995, **142**, 2577–2581.
39 H. C. Shiao, K. Chua, H. P. Lin, S. Slane and M. Salomon, *J. Power Sources*, 2000, **87**, 167–174.
40 J. Dong, Z. C. Zhang, Y. Kusachi and K. Amine, *J. Power Sources*, 2011, **196**, 2255–2259.
41 J. Bowers and I. A. McLure, *J. Chem. Soc., Faraday Trans.*, 1997, **93**, 265–271.
42 M. Mori, Y. Narukawa, K. Naoi and D. Futeux, *J. Electrochem. Soc.*, 1998, **145**, 2340–2348.
43 J. Y. Kim and D. Y. Lim, *Energies*, 2010, **3**, 866–885.
44 X. S. Huang, *J. Solid State Electrochem.*, 2011, **15**, 649–662.
45 Q. C. Zhuang, J. M. Xu, X. Y. Fan, Q. F. Dong, Y. X. Jiang, L. Huang and S. G. Sun, *Chin. Sci. Bull.*, 2007, **52**, 1187–1195.